Poster Presentations

Aerodynamic effects of dent holes on airfoils under subsonic and supersonic flow conditions

A.D.G Pathirana[1] and Geethal Siriwardana[2]

[1] Department of Mechanical and Automotive Engineering, Faculty of Engineering and Technology CINEC Campus, Malabe, Sri Lanka
[2] Department of Mechanical Engineering, Faculty of Engineering, University of Sri Jayewardenepura, Sri Lanka
[1]achaladpathirana@gmail.com
[2]geethal@sjp.ac.lk

Abstract. This research investigates the aerodynamic performance of airfoils in both subsonic and supersonic flows, focusing on the impact of non-symmetric and symmetric surface dents. Unlike previous studies that primarily considered symmetric or regularly spaced dimples, this study explores the effects of isolated dents—hemispherical, conical, and cylindrical—placed at various chordwise locations on both the upper and lower surfaces of the airfoil. Computational simulations were conducted using ANSYS Fluent. A total of 54 simulations were performed for a three-dimensional NACA 0012 airfoil under subsonic conditions, with Reynolds numbers ranging from 1.9×10^6 to 8.3×10^6 and angles of attack from $-12°$ to $+12°$. Additionally, nine two-dimensional simulations were carried out for a double-wedge airfoil at Mach number 3 to assess performance in the supersonic regime. The results demonstrate that the geometry, location, and surface area of dents significantly influence aerodynamic behavior. In subsonic flow, the highest lift-to-drag ratio of 49.6 was achieved with a hemispherical dent located at the mid-chord on the upper surface, indicating improved boundary layer control and delayed flow separation. In supersonic flow, a trailing dent placed at the leading edge of the lower surface generated lift even at zero angle of attack, doubling the lift-to-drag ratio compared to the clean airfoil. These findings were validated by benchmarking clean airfoil simulations against NASA's NACA 0012 data and existing literature, showing good agreement in pressure distribution and drag values. Overall, the study provides compelling evidence that non-symmetric dents can function as effective passive flow control mechanisms, with potential applications in UAVs, missiles, and other high-speed aerospace platforms.

Keywords: Airfoil Aerodynamics, Non-Symmetric Dimples, Passive Flow Control, Subsonic and Supersonic Flow, Computational Fluid Dynamics

1 Introduction

The aim of this study is to investigate the aerodynamic effect of such non-symmetric dent characteristics. By simulating dents of different shapes (conical, cylindrical, hemispherical), sizes, and positions along the airfoil chord, this work aims to understand how these localized geometric deviations affect lift, drag, and overall aerodynamic efficiency. A total of 54 three-dimensional simulations were performed on a NACA 0012 airfoil under subsonic conditions, with velocities ranging from 30 m/s to 130 m/s and angles of attack between −12° and +12°. To extend the work to high-speed regimes, nine two-dimensional supersonic calculations were conducted with a double-wedge airfoil at Mach number 3 as representative missile or high-speed wing sections. One particular region of interest in this research is the effect of non-symmetric dent placement on boundary layer behavior, separation, and, in supersonic flows, on geometry-local shockwave interaction. Through comparison of dented versus smooth surfaces, and through examination of lift-to-drag (L/D) ratios, the investigation tries to discern patterns and locations that would provide better aerodynamic performance via passive flow control. In the last several years, a number of studies have been conducted on the effect of dimples and surface modifications on the aerodynamic performance of airfoils. These investigations—both experimental and numerical—have covered a range of airfoil profiles, dimple geometries, and locations. Findings, however, vary from study to study, especially on whether the occurrence of dimples improves or worsens performance. Livya et al. [1] and Kaushik et al. [2] numerically studied a 3D symmetric NACA 0018 airfoil with various dimple geometries. Livya [1] tested semi-spherical, cylindrical, hexagonal, and compound dimples and determined that inward semi-spherical shapes gave maximum lift enhancement. Kaushik [2] found through his studies that both inward and outward dimples increased lift but also drag. Srivatsav [3] later confirmed with 2D and 3D simulations that outward dimples reduced drag in 2D, while in 3D, lift was increased at the expense of higher drag. Saraf et al. [4] tested on a NACA 0012 airfoil, testing 2D cases experimentally with dimples at different chordwise positions. The best performance was achieved when the dimple was positioned around 75% of the chord, which shows that position is crucial to the behavior of flow. Singh et al. [5] tested a NACA 0011 airfoil experimentally with different shapes and sizes of dimples and concluded that semi-cylindrical outward dimples of medium size positioned at 66% chord length performed optimally. In addition, Binci et al. [6] found that dimples on a NACA 64-014A airfoil reduced laminar separation and pressure drag, leading to enhancement of aerodynamic stability. On the contrary, Stolt et al. [7] reported performance losses caused by dimple application on a NACA 0015 airfoil, particularly in the leading-edge region. Zulkefli and MohdNur [8] tested dimples on a NACA 4415 profile and determined that inward and outward dimples were not effective near stall but that inward dimples gave marginal lift-to-drag benefits at moderate angles of attack. Mustak et al. [9] showed that both forms of dimples delayed stall by approximately 4° and improved lift and drag performance over the range of angles of attack. Further, Tej et al. [10] conducted a comparative CFD study of various 3D NACA airfoils and concluded teardrop-shaped inward dimples at 70% chord to be most effective, especially on more highly cambered airfoils. Some research has been conducted to improve flow control and delay in separation over airfoils. Siauw et al. [11] performed an experiment of pneumatic vortex generators on a NACA 0015 airfoil and noted a pressure-velocity signal correlation during the occurrence of flow separation at high attack angles. Niu et al. [12] performed dynamic stall behavior on a NACA 0012 airfoil and showed that a variable droop leading-edge can enhance aerodynamic performance. Also, conventional camber-changing devices like slats and flaps have been shown to increase lift [13]. Matsson et al. [14] took the NACA 2412 airfoil at low Reynolds numbers into account and found the stall angle to be somewhere between 14° and 16° by experiment and CFD investigation. Overall, these studies show that the dimple performance is a function of several parameters shape, size, location, and airfoil geometry. While some configurations enhance the lift and reduce the drag, others may worsen the performance. Such inconsistency brings out the need for exhaustive parametric studies like the current work, which addresses non-symmetric dents in subsonic flow. Supersonic aerodynamics studies recently have focused on the impact of surface geometry changes on shock behavior and aerodynamic performance. Hodson et al. [15] and Manshadi & Aghajanian [16] demonstrated that optimal airfoil shapes have the potential to maximize lift-to-drag performance by reducing shock. Hari et al. [17] showed that small surface intersections can have a profound influence on shockwave interactions. Together, these papers confirm that supersonic flow can be passively manipulated by local surface features—i.e., dents or dimples. This work builds upon that foundation by investigating non-symmetric dent geometries as a passive means to control shock-boundary interactions and improve aerodynamic efficiency. Ajay Varma [18] formulated Pressure Coefficient is found to decrease with increase in Mach number after the shock. Maximum Mach number and turbulent kinetic energy over the surface is found to increase with inlet Mach number. Aminjan et al. [19] conducted a CFD (Computational Fluid Dynamics) simulation of thick double-wedge airfoils at Mach number 2. The research is likely to have been aimed at the study of aerodynamic characteristics of such airfoils under the condition of supersonic flow at a Mach number of 2 and could have studied the effect of airfoil thickness on the flow pattern. Ferrari developed an analytical theory in 1958 to calculate wave drag for thin double-wedge airfoils [20]. The theory provides a way of understanding and predicting the drag behavior of such airfoils at supersonic velocities. The most significant aspect of the theory is its consideration of the wave drag as a significant contributor to overall drag at supersonic velocities due to the formation of shock waves. This work adds to a clear void in published research for utilizing previous studies and examining non-symmetric dents on 2D and 3D airfoils under subsonic and supersonic conditions. This situates this research in a special position of contributing innovative insights to passive flow control and aerodynamic surface development.

The findings not only reveal the mechanisms by which surface damage can lead to decreased performance but also mechanisms by which strategically located dents can increase lift or reduce drag a potential concept for UAVs, missiles, and high-speed applications where the use of external control devices is undesirable. This study bridges the gap between idealized control of airflow and real geometric defects.

2 Computational Methodology

This study investigates the aerodynamic influence of surface dents on airfoils under both subsonic and supersonic conditions using Computational Fluid Dynamics (CFD) in ANSYS Fluent. The NACA 0012 airfoil for the subsonic case and double-wedge airfoil for the supersonic case were considered. Various dimple geometries—symmetric and non-symmetric geometries were explored using surface geometry modification and the calculation of lift, drag, and flow structure. In the subsonic simulations, dent diameters were varied between (1–10) % of the chord length, with depths ranging from (0.3-1) % of the chord. These ranges were chosen to capture shallow dents as well as deeper configurations that could act as passive flow-control devices. The purpose of this variation was to investigate whether dent size influences laminar–turbulent transition, flow separation, and stall delay.

Governing Equations The computational analysis of airflow over the dented airfoils was performed by solving the Reynolds-Averaged Navier-Stokes (RANS) equations along with the Shear Stress Transport (SST) k–ω turbulence model in ANSYS Fluent. These equations govern the conservation of mass, momentum, and turbulence transport. All equations were solved in steady-state form, using a second-order discretization scheme
Continuity equation;

$$\partial u/\partial x + \partial v/\partial y + \partial w/\partial z = 0 \quad (1)$$

Momentum equations;

$$\rho(u\ \partial u/\partial x + v\ \partial u/\partial y + w\ \partial u/\partial z) = -\partial p/\partial x + \mu\nabla^2 u \quad (2)$$

$$\rho(u\ \partial v/\partial x + v\ \partial v/\partial y + w\ \partial v/\partial z) = -\partial p/\partial y + \mu\nabla^2 v \quad (3)$$

$$\rho(u\ \partial w/\partial x + v\ \partial w/\partial y + w\ \partial w/\partial z) = -\partial p/\partial z + \mu\nabla^2 w \quad (4)$$

k-equation:(turbulence kinetic energy);

$$\partial(\rho k)/\partial t + \nabla\cdot(\rho kV) = Pk - \beta^*\rho k\omega + \nabla\cdot[(\mu + \sigma k\mu t)\ \nabla k] \quad (5)$$

ω-equation:(specific dissipation rate);

$$\partial(\rho\omega)/\partial t + \nabla\cdot(\rho\omega V) = \alpha(\omega/k)P_k - \beta\rho\omega^2 + \nabla\cdot[(\mu + \sigma_\omega\mu_t)\,\nabla\omega \quad (6)$$

Nomenclatures: u, v, z are the components of velocity vector in x, y, z-components ρ= air density, μ= dynamic viscosity, Pk = production term of k, ∇= velocity vector, α, β, σk, σω= empirical constants derived from calibration.

2.1 Subsonic Methodology

Mesh Sensitivity Analysis A mesh independence test was conducted to ensure accurate aerodynamic predictions for the subsonic 3D NACA 0012 airfoil. Three meshes of increasing density, containing approximately 400,000, 500,000, and 800,000 elements, were generated and tested at 50 m/s and 0° angle of attack (AoA). Inflation layers were applied near the airfoil surface to resolve the boundary layer, with the first cell height adjusted to achieve $y^+ < 1$, ensuring compatibility with the SST k–ω turbulence model. Lift and drag coefficients were computed for each mesh and compared to evaluate convergence. Minimal variation (<4%) was observed beyond 500,000 elements, confirming that further refinement did not significantly affect the results. Based on this analysis, the finest mesh of 800,000 elements was adopted for all subsonic simulations.

Computational Setup A 3D model of NACA 0012 airfoil with a chord length and span of 1 meter was prepared. Hemispherical, cylindrical, and conical shaped surface dents of different depths and diameters were developed and introduced at various chordwise from leading edge to trailing edge positions on upper and lower surfaces.
The computational domain was stretched, vertical height 8 and horizontal height 12 lengths to offer undisturbed flow. An unstructured tetrahedral mesh was generated, such as inflation layers next to the airfoil surface. The boundary conditions were a uniform velocity inlet (30–130 m/s), pressure outlet 0 Pa, symmetry side surfaces, and a no-slip airfoil wall. The simulations used the pressure-based solver with SST k–ω turbulence model, which is capable of simulating boundary layer separation and near-wall effects. Second-order discretization schemes were used, and simulations were run until residuals fell below 10^{-5} and aerodynamic forces converged. Reynolds numbers ranged between 1.91×10^6 and 8.29×10^6, which were dependent on inlet velocity

Simulation Parameters

Table 1. Simulation case setup for NACA 0012 airfoil.

Case No	Reynolds Number	Dent shape	Dimple diameter (D/C)	Dimple depth (d/D)	Placement (%Chord)	AoA (·)
1-4	1.91×10^6	-	-	-	-	-4,0,4,12
5	6.38×10^6	-	-	-	-	-8
6	7.65×10^6	H S(N-S)	0.01	0.3	L E	12
7-11	1.91×10^6	H S(N-S)	0.01	0.3	L E	-8, -4,0,4 8
12-16	6.38×10^6	H S(S)	0.1	0.5	M C	-4,0,4,8 12
17	4.46×10^6	H S(S)	0.1	0.5	M C	-8
18-22	1.91×10^6	H S(N-S)	0.05	0.333	T E	-4,0,4,8 12
23	3.19×10^6	H S(N-S)	0.05	0.333	T E	-12
24-26	3.19×10^6	H S(N-S)	0.01	1	L E(L-S)	-8,0,8
27-30	3.19×10^6	CO(N-S)	0.05	0.5	L E	-4,0,4,12
31	4.46×10^6	CO(N-S)	0.05	0.5	L E	-12
32-35	6.38×10^6	CO(S)	0.05	0.5	M C	-8,0,8,12
36	8.29×10^6	CO(S)	0.05	0.5	M C	-12
37-38	1.91×10^6	CO(N-S)	0.01	0.1	T E	4,8
39	6.38×10^6	CO(N-S)	0.01	0.1	T E	0
40	1.91×10^6	CO(N-S)	0.01	0.1	T E	-4
41	4.46×10^6	CO(N-S)	0.01	0.1	T E	-8
42-45	6.38×10^6	CO(S)	0.05	0.5	M C(L-S)	-4,0,4,4
46	6.38×10^6	CY(B-C)	0.05	1.5	L E	0
47	6.38×10^6	-	-	-	-	8
48	1.91×10^6	H S(N-S)	0.01	0.1	T E(L-S)	0
49	6.38×10^6	CY(B-C)	0.05	0.52	M C	0
50	1.91×10^6	CY Hole	0.01	6	L E	0
51-54	6.38×10^6	CY(B-F)	0.05	0.2	T E	-12, -8,0,12

Nomenclatures :C=chord length, H S=Half spherical, CO=conical, CY=Cylindrical, N-S=non-symmetric, S= symmetric, B-C= bottom curve, B-F= bottom flat, L E= Leading edge, M C= Mid chord, T E= Trailing edge, L-S= lower surface

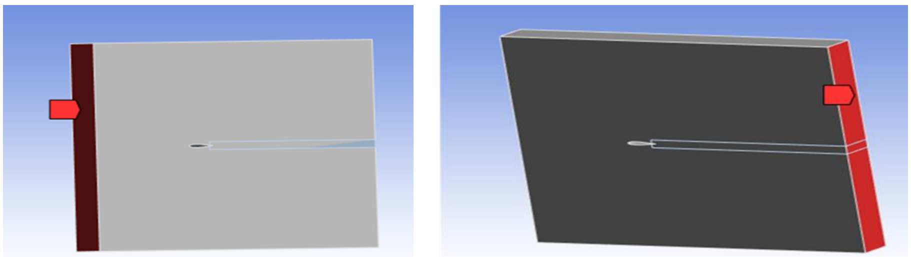

(a) (b)

Fig. 1. Boundary conditions (a) inlet (b) outlet

2.2 Supersonic Methodology

For the supersonic simulation, a 2D double-wedge airfoil of 2 meters chord length and 0.3 meters height was simulated. Mesh density was increased at leading edges and dimple locations to capture shock interactions accurately. Boundary conditions were defined as a supersonic inlet (Mach number 3), pressure outlet, and inviscid slip wall boundary on the surface of the airfoil.

Two simulation approaches were utilized. First, an inviscid flow simulation was used to study generic shock wave structures and surface pressure effects. Second, particular cases were simulated using a viscous setup with the SST k–ω model of turbulence to account for boundary layer flow effects. The solver was run at compressible flow conditions with coupled formulations, with convergence ensured through monitoring drag, lift, and residual stability.

Table 2. Supersonic simulation setup parameters for double wedge airfoil

Case No	Mach No	Dent shape	Dimple diameter(m)	Dimple depth(m)	Placement	Turbulence Model	AoA (·)
1	3	-	-	-	-	Inviscid	0
2	3	S C(S)	0.009	0.009	L E(U-S)	Inviscid	0
3	3	S C(S)	0.01	0.01	L E(L-S)	Inviscid	0
4	3	T (S)	0.003	0.003	L E(L-S)	Inviscid	0
5	3	S C(S)	0.009	0.009	L E(U-S)	Inviscid	0
6	3	T (NS)	0.01	0.01	L E(L-S)	Inviscid	0
7	3	T (NS)	0.02	0.02	L E(L-S)	Inviscid	0
8	3	T (NS)	0.003	0.003	L E(L-S)	Inviscid	0
9	3	T (NS)	0.01	0.01	L E(L-S)	SST k–ω	4

Nomenclatures: S C= Semi-circle, T= Triangular, S= symmetric, NS= Non-symmetric, L E= Leading edge, U-S= upper surface, L-S= lower surface

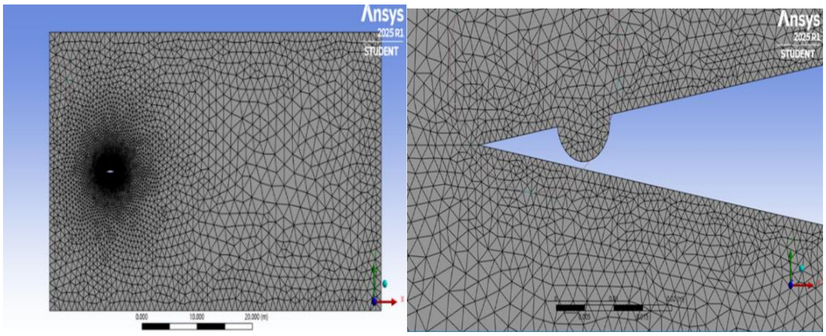

(a) **(b)**

Fig. 2. Mesh configuration (a) Airfoil (b) Around dimple

3 Results and Discussion

3.1 Subsonic Regime

Among the modified geometries, the symmetric conical dimple at mid-chord (Case 15) showed the most aerodynamically superior performance with Cl = 0.8 and Cd = 0.017 at 4° AoA, with a Cl/Cd ≈ 49.6 superior to the smooth and other dimpled geometries. Similarly, the asymmetric half spherical dimple at the leading edge lower (Case 26) produced Cl = 0.85 and Cd = 0.019, yielding a lift-to-drag ratio of 44.54 at 8° AoA. Both cases confirmed that carefully designed dimples shallow and placed strategically can maintain or improve aerodynamic efficiency without active control mechanisms. On the other hand, cylindrical dimples, particularly curve-bottomed and deep dimples, incurred aerodynamic penalties. Case 50, for example, had negative lift (Cl = –0.017) and moderate Cd, meaning that such configurations destabilize the boundary layer and promote premature separation. Even the flat-bottom cylindrical dimple at the trailing edge (Case 23), though better, was worse than conical counterparts.

Comparison of Baseline Airfoil (smooth NACA 0012) with special dented cases of each AoA

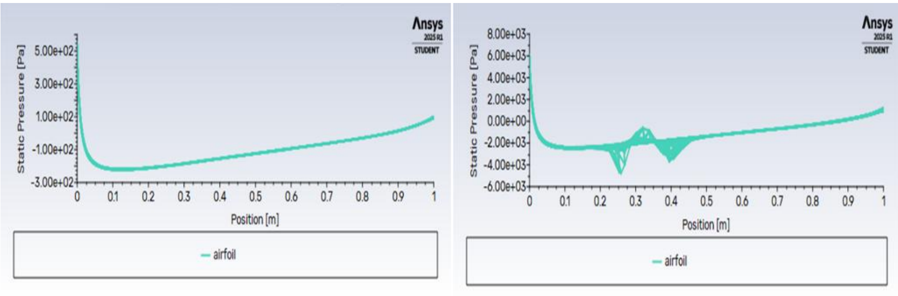

(a) **(b)**

Fig. 3. Static pressure (a)baseline airfoil, (b) conical symmetric dent shape airfoil

According to Fig. 3, (a) Static pressure is symmetrically distributed along the chord. Maximum pressure is located near stagnation point at leading edge. Pressure drops off quickly over both surfaces indicating initial acceleration, with no asymmetry due to zero AoA.(b) Pressure plot shows localized regions of increased pressure recovery near the dimple. A noticeable high-pressure buildup is seen in front of the dimple due to flow stagnation and flow redirection, forming a mini shock-like effect even in subsonic flow. Pressure is relatively lower downstream of the dimple, suggesting flow reattachment and reduced separation or vortex formation.

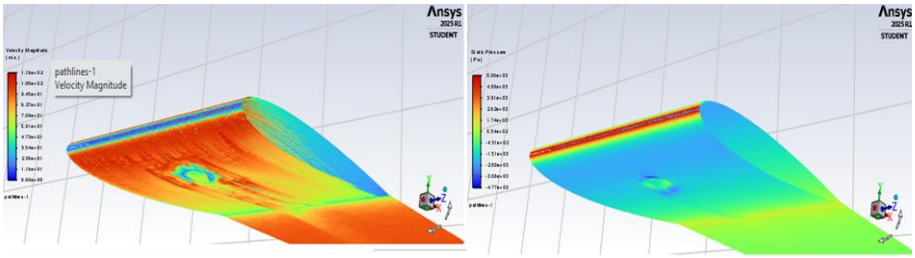

(a) **(b)**

Fig. 4. (a) velocity magnitude, (b) static pressure

According to Fig. 4, (a) The dent imposes a local velocity gradient close to the surface. In the dented form, observed slight flow acceleration over the dimple due to local curvature and flow constriction. This imposes slight suction on the upper surface and a positive pressure gradient that has to enhance L/D ratio by managing boundary layer growth. (b) A visible low-pressure region is formed around the dimple location, which enhances suction. The local depression generates a marginal lift gain and a boundary layer energizing effect that reduces flow separation. As a result, drag is also decreased.

3.2 Supersonic Regime (Comparative Efficiency Based on L/D Ratio)

L/D ratio is a most critical performance metric of aerodynamics. In current dataset, the smooth airfoil (Case 1), in Table 2 yielded L/D ≈ 0 while Case 3 yielded an improved L/D ≈ 0.81 and case 7, L/D= 2.005 at the expense of adding a passive flow control geometry.
Supreme case (Case 7): lower surface triangular dimple, Cd =0.083, Cl =0167, L/D = 2.004, Worst case (Case 5): upper surface dimple degraded both lift and drag
Baseline (Case 1): near zero lift, reasonable drag.

Pressure, velocity contours variation with baseline & dimpled cases of double wedged airfoil

According to Fig.5(a)normal oblique shock structures form at the leading edge of the wedge surfaces. Flow is symmetric: pressure distribution on upper and lower surfaces is the same. (b)Acceleration behind the leading edge is linear followed by smooth deceleration in the downstream zone. No vortex structures or flow separation are seen.

This is what should be expected for idealized supersonic flow over sharp-edged bodies

(c) Asymmetric pressure distribution is established higher pressure on top surface than at bottom contributing to net positive lift. Shock wave of the dimple appears shallow and well-contained, keeping pressure drag to a minimum. (d)Velocity increases a bit near the dimple, indicating localized acceleration. Flow is attached with no sign of a separation bubble. A vortex or recirculation zone is indicated by a change in velocity gradient downstream of the dimple. The triangular shape creates passive flow control, re-energizing the boundary layer at little cost in drag. This result is in line with passive vortex generator theory in the supersonic regime boosting Cl without great shock costs, producing an improved L/D. (e) Pressure drop due to the dimple does occur, albeit diffused with respect to Case 6.A smaller pressure gradient is formed across the airfoil. There is some asymmetry but no significant favorable pressure gradient subsequent to the dimple.

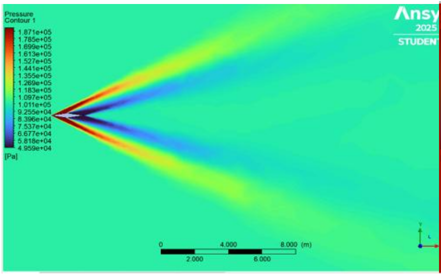
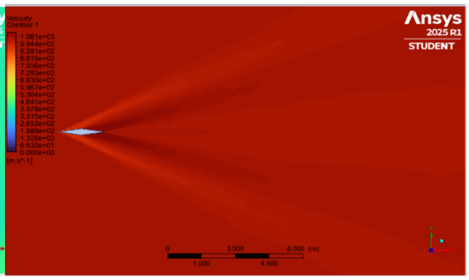

(a) **(b)**

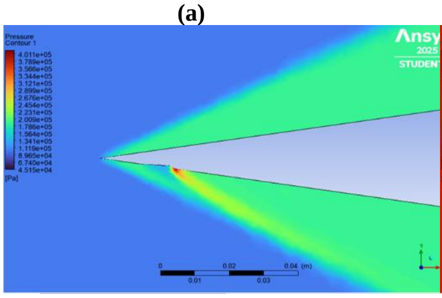
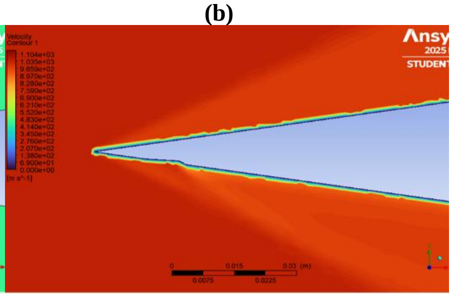

(c) **(d)**

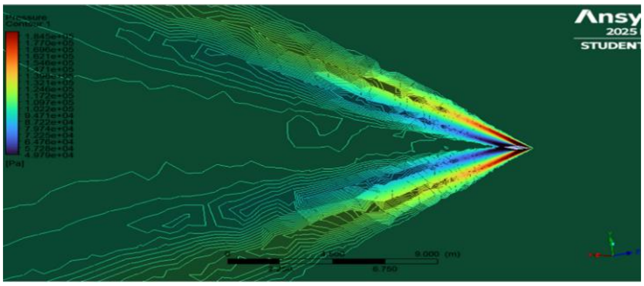

(e)

Fig. 5. (a) pressure contour of baseline airfoil, (b) velocity contour of baseline airfoil, (c) pressure near dimple area (case 6),
(d) velocity around dimple area (case 6), (e) pressure contour of (case 2)

4 Conclusions

This study completely explored the aerodynamic impact of symmetric and non-symmetric dent holes on airfoils under subsonic and supersonic flow. 54 subsonic CFD runs on a 3D NACA 0012 airfoil with variation of dent shape, size (diameter and depth), and location along the chord were conducted. In the supersonic regime, nine 2D runs on a double-wedge airfoil at Mach number 3 examined the impact of corresponding geometric perturbations on shockwave formation and aerodynamic coefficients. The results confirmed that some of the dent configurations could enhance lift-to-drag ratio (L/D), verifying the aerodynamic potential of passive geometric control. The best performing subsonic case 15 with half spherical mid-chord dimple registered a Cl/Cd ratio of 49.6, while Case 26 (an asymmetric half-spherical dimple at lower leading edge) registered a ratio of 44.5. Supersonic computation also showed encouraging performance improvement, especially in Case 7, which significantly enhanced L/D ratio double over the baseline.

These findings validate that localized, shallow surface dents especially those positioned near the leading or mid-chord locations can have beneficial effects on flow behavior independently of active control mechanisms. The research hence advocates for the application of non-symmetric dimples as a passive approach to enhancing aerodynamic efficiency under both low-speed and high-speed flight conditions. Current and future work ought to advance viscous supersonic simulations, wind tunnel tests, and multi-objective optimization of dent geometries for practical applications in aerospace engineering.

References

1. E. Livya, G. Anitha and P. Valli, Aerodynamic Analysis of Dimple Effect on Aircraft Wing, International Journal of Aerospace and Mechanical Engineering, 9(2), pp. 350-353, 2015.
2. V. Kaushik, M. Mahore and S. Patil, Analysis of Dimpled Wing of an Aircraft, International Journal of Engineering Development and Research, 6(3), 2018.
3. D. Srivastav, Flow Control over Airfoils using Different Shaped Dimples, International Conference on Fluid Dynamics and Thermodynamics Technologies, Singapore, 2012.
4. A. K. Saraf, M. P. Singh, T. S. Chouhan, Effect of Dimple on Aerodynamic Behaviour of Airfoil, International Journal of Engineering and Technology, 9(3), pp. 2268-2277, 2017.
5. D. Singh, R. H. Gajghat, M. K. Manik, Experimental Investigation to Examine the Effect of Shape and Size of Dimple at Suction Surface of Aerofoil, International Journal of Scientific & Technology Research, 8(12), pp. 521-534, 2019.
6. L. Binci, G. Clementi, V. D'Alessandro, S. Montelpare and R. Ricci, Study of the flow field past dimpled aerodynamic surfaces: numerical simulation and experimental verification, 35th UIT Heat Transfer Conference, Ancona, Italy, 2017.
7. A. J. Stolt, A. H. Ullah and J. Estevadeordal, Study of Leading-Edge Dimple Effects on Airfoil Flow Using Tomographic PIC and Temperature Sensitive Paint, Fluids, 4(4), 2019.
8. N. F. Zulkefli, W. K. F. W. Samsudin and N. M. Nur, Dimples Effectiveness on Naca4415 Airfoil, International Journal of Advanced Science and Technology, 29(6), pp. 203-207, 2020.
9. R. Mustak, N. Uddin, MD. and M. Mashud, Effect of different shaped dimples on airfoils, Proceedings of the International Conference on Mechanical Engineering and Renewable Energy, Chittagong, Bangladesh, 2015.
10. G. R. Tej, B. Rajasai and S. Anurang, Variation of Behaviour of Dimples on Aircraft Wings, IEEE Aerospace Conference, Big Sky, Montana, 2016.
11. Attenuation of Shock Induced Separation, Int. J. Appl Sci Technol, 2(3), pp 34-52, 2012.
12. W. L. Siauw and J. P. Bonnet, Transient phenomena in separation control over a NACA 0015 airfoil, Int.J. Heat Fluid Flow, 67, pp 23-29, 2017.
13. J. Niu, J. Lei, T. Lu, Numerical research on the effect of variable droop leading-edge on oscillating NACA 0012 airfoil dynamic stall, Aerospace Science and Technology, 72, pp 476–485, 2018.
14. S. Mahon, X. Zhand, Computational analysis of pressure and wake characteristics on an aerofoil in ground effect, ASME, 127, pp 290-298, 2005.
15. J. D. Hodson, A. P. Christopherson, J. D. Deaton, A. M. Pankonien, G. W. Reich, P. S. Beran, Aeroelastic topology optimization of a morphing airfoil in supersonic flow using evolutionary design. AIAA Scitech Forum, 2019.
16. N. Hari, J. A. Schetz, R. K. Kapania, Numerical prediction of interference drag of a strut-surface intersection in supersonic flow, AIAA Scitech Forum, 2019.

17. [17] Manshadi MD, Aghajanian S (2018) Computational aerodynamic optimization of wing-design concept at supersonic conditions by means of the response surface method. J Braz Soc Mech Sci Eng 40(5):254–265
18. A. Varma, Aerodynamic Analysis Over Double Wedge Airfoil, IOP Conference Series Materials Science and Engineering, 197(1):012076, 2017.
19. Aminjan, Aerodynamic Analysis of Double Wedge Airfoil in Different Angle of Attack at Supersonic Flow, Solid State Technology, 63(6):14417-14428, 2020.
20. C. Ferrari, Analytical prediction of wave drag for double-wedge airfoils. Journal of the Aeronautical Sciences, 25(10), pp.662–664, 1958.